LEAST SQUARES IMAGE MATCHING for CE604

J. Bethel

14 June 1997

1 Introduction

In the conventional approach to least squares image matching, we model the correspondence between two image fragments by a geometric model (six parameter transformation) and a radiometric model (two parameter transformation). Pixel gray values in one image are arbitrarily chosen to be the observables, while pixel gray values in the other image are chosen to be constants. Figure 1 shows an enlarged, ideal image of a cross, with the pixel boundaries delineated for clarity. Figure 2 shows another depiction of the same cross, having been transformed by scale, rotation, and translation. This image pair, although simulated, will be used to illustrate the least squares matching techniques between, for example, fragments from the left and right images of a stereo pair.

For further clarification, Figure 3 shows the grid pattern used in resampling the ideal cross in order to produce the transformed cross. It illustrates the point that, geometric transformations applied to produce a resampling grid result in the opposite effects in the visible objects after resampling. For example, shrinking the grid enlarges the objects, rotating the grid one way rotates the objects the other way, shifting the grid one way shifts objects the other, etc. Knowing the a priori coordinate relationships between these two simulated images should allow verification of the least squares matching results.

Experience has shown that the alignment/correspondence between two images to be matched generally has to be within a few pixels or the process will not converge. This is more restrictive than other matching methods, and therefore forces one to use least squares methods only for *refinement* rather than *from scratch* processing of new imagery. On the other hand, performing least squares matching at the high (small) end of the image pyramid and working progressively downward could provide a way to process images with poorer alignments.

If for some reason the geometric relationship between the images is not consistent with the usually applied six parameter model, then the model would have to be expanded. Up to now this has not proven necessary in photogrammetric applications.

Also note that nothing in the conventional approach to least squares matching enforces any constraints from the, possibly known, photogrammetric orientation. One could, for example, constrain the shift parameters so that they are only allowed to move in the epi-polar direction.

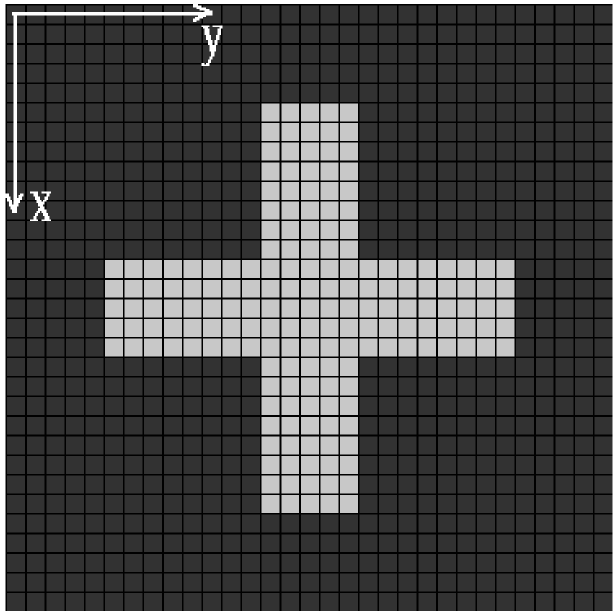

Figure 1: Ideal Cross Image, g(x,y), treated as Left

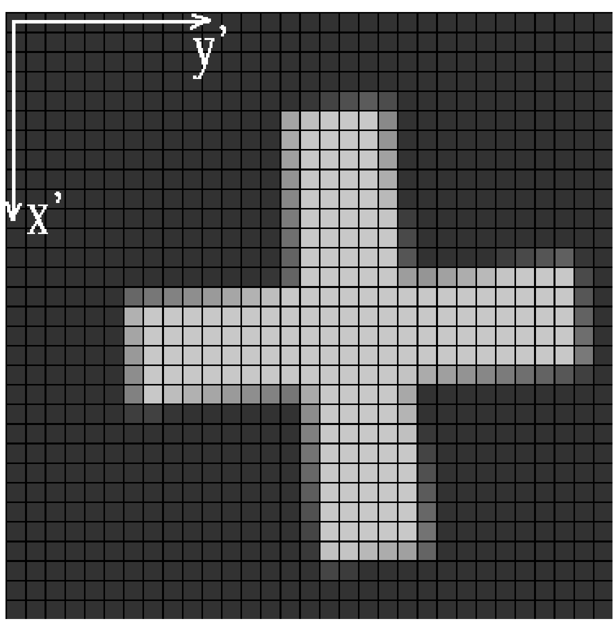

Figure 2: Rotated Cross Image, h(x',y'), treated as Right

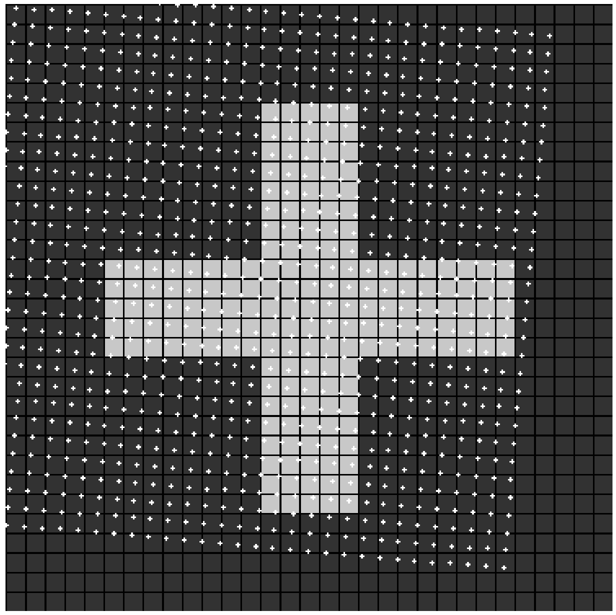

Figure 3: Resampling Grid to Produce the Rotated Cross

2 Derivation

A simplified condition equation, considering only the geometric parameters would be,

$$g(x, y) = h(x', y') \tag{1}$$

in which the two coordinate systems are related by the six parameter transformation,

$$\begin{aligned} x' &= a_1 x + a_2 y + a_3 \\ y' &= b_1 x + b_2 y + b_3 \end{aligned} \tag{2}$$

An extended model including two radiometric parameters for contrast and brightness (or equivalently gain and offset) would be,

$$g(x, y) = k_1 h(x', y') + k_2 \tag{3}$$

Written in the form of a condition equation it becomes,

$$F = g(x, y) - k_1 h(x', y') - k_2 = 0 \tag{4}$$

in which the the parameters are $a_1, a_2, a_3, b_1, b_2, b_3, k_1$, and k_2, g represents the observation, x, y are constants, and h is a constant. This equation can be linearized into the form,

$$\mathbf{v} + \mathbf{B}\boldsymbol{\Delta} = \mathbf{f} \tag{5}$$

Since we assume that the images are nearly aligned and are radiometrically similar, we can take the initial approximation parameter vector to be,

$$\begin{bmatrix} a_1^o \\ a_2^o \\ a_3^o \\ b_1^o \\ b_2^o \\ b_3^o \\ k_1^o \\ k_2^o \end{bmatrix} = \begin{bmatrix} 1 \\ 0 \\ 0 \\ 0 \\ 1 \\ 0 \\ 1 \\ 0 \end{bmatrix} \tag{6}$$

The coefficients of the **B** matrix will consist of the partial derivatives of Equation(4).

$$\mathbf{B} = \begin{bmatrix} \frac{\partial F}{\partial a_1} & \frac{\partial F}{\partial a_2} & \frac{\partial F}{\partial a_3} & \frac{\partial F}{\partial b_1} & \frac{\partial F}{\partial b_2} & \frac{\partial F}{\partial b_3} & \frac{\partial F}{\partial k_1} & \frac{\partial F}{\partial k_2} \end{bmatrix} \tag{7}$$

These can be developed as follows,

$$\frac{\partial F}{\partial a_1} = -k_1 \frac{\partial h}{\partial a_1} = -k_1 \frac{\partial h}{\partial x'} \frac{\partial x'}{\partial a_1} = -h_x x \tag{8}$$

where we evaluated the expression at the initial approximations, and for notational compactness we adopt,

$$\begin{aligned} h_x &= \tfrac{\Delta h}{\Delta x} \approx \tfrac{\partial h}{\partial x} \\ h_y &= \tfrac{\Delta h}{\Delta y} \approx \tfrac{\partial h}{\partial y} \end{aligned} \tag{9}$$

In practice, these are computed as follows using gray values from the right image,

$$\begin{aligned} h_x &= \tfrac{h(x'+1,y')-h(x'-1,y')}{2} \\ h_y &= \tfrac{h(x',y'+1)-h(x',y'-1)}{2} \end{aligned} \tag{10}$$

Note that h_x represents a derivative, whereas $h(x', y')$ represents a gray value in the right image.

$$\frac{\partial F}{\partial a_2} = -k_1 \frac{\partial h}{\partial a_2} = -k_1 \frac{\partial h}{\partial x'} \frac{\partial x'}{\partial a_2} = -h_x y' \tag{11}$$

$$\frac{\partial F}{\partial a_3} = -k_1 \frac{\partial h}{\partial a_3} = -k_1 \frac{\partial h}{\partial x'} \frac{\partial x'}{\partial a_3} = -h_x \tag{12}$$

By similar analysis,

$$\frac{\partial F}{\partial b_1} = -h_y x' \tag{13}$$

$$\frac{\partial F}{\partial b_2} = -h_y y' \tag{14}$$

$$\frac{\partial F}{\partial b_3} = -h_y \tag{15}$$

$$\frac{\partial F}{\partial k_1} = -h(x', y') \tag{16}$$

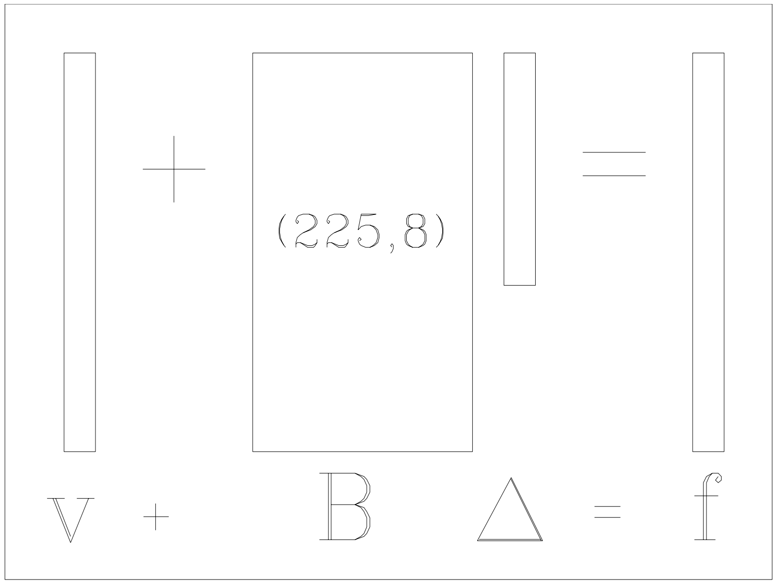

Figure 4: Condition Equations for 15 by 15 Window

$$\frac{\partial F}{\partial k_2} = -1 \tag{17}$$

The f term, the righthand side term, is,

$$f = -F = -(g(x,y) - k_1 h(x',y') - k_2) \tag{18}$$

evaluated at the approximations (the identity transformation), it becomes,

$$f = h(x,y) - g(x,y) \tag{19}$$

As an example, for a 15 by 15 size window the condition equations would appear as in Figure 4. It is assumed that the surrounding border pixels are available for computing the partial derivatives for the data in Figure 4. This would allow a condition equation to be written for *each* pixel within the 15 by 15 window, i.e. with no special considerations for those on the edges.

The resulting normal equations may be formed sequentially, avoiding the *actual formation* of the full condition equations. They are then solved for the parameter corrections. For the second and subsequent iterations, we resample the right image, $h(x',y')$ using the *inverse* transformation defined by the updated six parameters. This is necessary because, as mentioned earlier, transformation effects on the resampling grid produce the opposite effects on the objects visible after resampling. After several iterations and resamplings, the two images should appear to be aligned and registered. Following are a few practical hints.

- Update parameters just like nonlinear least squares, i.e. $a^1 = a^0 + \delta a$
- Convergence occurs when $\Delta \rightarrow 0$
- the **B** matrix and **f** vector are computed from the resampled right image
- The right image is resampled for every iteration following the first, usually by bilinear interpolation

3 References

1 Ackermann, F., (1983), "High Precision Digital Image Correlation", *Proceedings 39th Photogrammetric Week*, Institut für Photogrammetrie, Universität Stuttgart, Stuttgart, GER, Heft 9.

2 Ackermann, F., (1988), "Digital Image Correlation: Performance and Potential Application in Photogrammetry", presented at Thompson Symposium, Birmingham.

3 Arnold, R., (1978), "Local Context in Matching Edges for Stereo Vision", *Proceedings: Image Understanding Workshop*, Cambridge, MA, pp. 65-72.

4 Ayache, N. and Faverjon, B., (1987), "Efficient Registration of Stereo Images by Matching Graph Description of Edge Segments", *International Journal of Computer Vision*, pp. 107-131.

5 Baker, H, and Binfford, T., (1981), "Depth from Edge and Intensity Based Stereo", *Seventh International Joint Conference on Artificial Intelligence*, Vancouver, BC., pp. 631-636.

6 Barnard, S., and Fischler, M., (1982), "Computational Stereo", *ACM Computing Surveys*, Vol. 14, No. 4, pp. 553-572.

7 Barnard, S., (1987), "Stereo Matching by Hierarchical Microcanonical Annealing", *Technical Note No. 414*, SRI International, Menlo Park, USA.

8 Benard, M., Boutaleb, A., Kölbl, O., and Penis, C., (1986), "Automatic Stereophotogrammetry: Implementation and Comparison of Classical Correlation Methods and Dynamic Programming Based Techniques", *Proceedings ISPRS Comm. III Symposium*, Rovaniemi, Finland.

9 Burt, P., (1980), "Fast, Hierarchical Correlations with Gaussian-like Kernels", *University of Maryland Computer Science Center Report, TR-860.*

10 Förstner, W., (1982), "On the Geometric Precision of Digital Correlation", *Proceedings of ISPRS Com. III Symposium*, Helsinki, pp. 176-189.

11 Förstner, W., (1984), "Quality Assessment of Object Location and Point Transfer Using Digital Image Correlation Techniques", Proceedings of ISPRS Congress, Com. III, Rio de Janeiro, pp. 197-219.

12 Förstner, W., (1986), "A Feature Based Correspondence Algorithm for Image Matching", *Proceedings ISPRS Comm. III Symposium*, Rovaniemi, Finland.

13 Gülch, E., (1988), "Results of Test on Image Matching of ISPRS WG III/4", *Proceedings of ISPRS Congress, Com. III*, Tokyo.

14 Hannah, M., (1987), *Test Results from SRI's Stereo System*, SRI International, Menlo Park, USA.

15 Hannan, M., (1988), "Digital Stereo Image Matching Techniques", *Proceedings of ISPRS Congress, Com. III*, Tokyo, p. 280.

16 Helava, U., (1988), "Object Space Least Squares Correlation", *Proceedings of ISPRS Congress, Com. III*, Tokyo, pp. 321-331.

17 Henriksen, K., (1986), *Feature Based Stereo Matching*, Technical Report DIKU-86-7, Computer Science Department, University of Copenhagen, Copenhagen, Denmark.

18 Li, M. (1988), "High Precision Relative Orientation Using the Feature Based Matching Techniques"

19 Marr, D. and Poggio, T., (1976), "Cooperative Computation of Stereo Disparity", *Science*, Vol. 194, pp. 283-287.

20 Moravec, H., (1980), *Obstacle Avoidance and Navigation in the Real World by a Seeing Robot Rover*, Ph.D. Thesis, Stanford University, Computer Science Department Report STAN-CS-80-813.

21 Norvelle, R., (1981), *Interactive Digital Correlation Techniques for Automatic Compilation of Elevation Data*, U.S. Army Engineer Topographic Laboratories, ETL-0272.

22 Ohta, Y., and Kanade, T., (1985), "Stereo by Intra- and Inter-Scanline Search Using Dynamic Programming", *IEEE Transactions on Pattern Analysis and Machine Intelligence*, Vol. PAMI-7, No. 2, pp. 139-154.

23 Panton, D., (1978), "A Flexible Approach to Digital Stereo Mapping", *Photogrammetric Engineering and Remote Sensing*, Vol. 44, No. 12, pp. 1499-1512.

24 Pollard, S., Mayhew, J., and Frisby, J., (1985), "PMF: A Stereo Corresspondence Algorithm Using a Disparity Gradient Limit", *Perception*, Vol. 14, pp. 449-470.

25 Price, K., (1985), "Relaxation Matching Techniques - A Comparison", *IEEE PAMI-7*, No. 5.

26 Quam, L., (1984), "Hierarchical Warp Stereo", *Proceedings: Image Understanding Workshop*, New Orleans, pp. 149-156.

27 Rosenholm, D. (1987), "Multi-Point Matching Using the Least Squares Technique for Evaluation of Three-Dimensional Models", *Photogrammetric Engineering and Remote Sensing*, June, pp.621-626.

28 Thurgood, J. and Mikhail, E., (1982), *Subpixel Mensuration of Photogrammetric Targets in Digital Images*, Purdue University School of Civil Engineering Report, CE-PH-82-2i.

29 Wrobel, B., (19XX), "Facets Stereo Vision (Fast Vision) - A New Approach to Computer Stereo Vision and to Digital Photogrammetry", *Proceedings ISPRS Intercommission Workshop*, Interlaken.